

Elastic properties of magnetostrictive thin films using bending and torsion resonances of a bimorph

Zs. Sárközi^{a)}

Babeş-Bolyai University, Physics Department, Str. Kogălniceanu 1, Cluj-Napoca 3400, Romania

K. Mackay and J. C. Peuzin

Laboratoire de Magnétisme Louis Néel, CNRS, BP 166, 38042-Grenoble, France

(Received 3 April 2000; accepted for publication 23 August 2000)

The modification of the elastic properties of giant magnetostriction alloy films due to an applied magnetic field (the ΔE effect), has been studied. Two different types of films were deposited on Si substrates: (i) single layers of TbDyFeCo alloys typically 1000 nm thick and (ii) nanocomposite multilayer films of FeCo/TbFeCo each having a typical thickness of 6 nm. Both types of films were rendered magnetically anisotropic with a well defined in-plane easy axis. Rectangular samples were cut out of these bimorphs and firmly glued at one end to a heavy base to form a simple cantilever structure. The variations of film elastic moduli were deduced from the shifts of the cantilever resonance frequencies as a function of bias field for two basic configurations: (i) field applied along the easy axis and (ii) field applied along the hard axis. In contrast with previous work, both flexural and torsion resonance modes were excited and studied. As a result the field induced variations of both planar traction modulus and the shear modulus were obtained and new interesting features were discovered. In particular strongly negative values of the shear modulus were observed (at least in the nanocomposite films) in the vicinity of the divergence in the transverse magnetic susceptibility at saturation field along the hard axis. A simple but complete theoretical analysis shows that the uniaxial anisotropy model together with the assumption of isotropic magnetoelastic coupling gives a good semiquantitative understanding of all the experimental results. © 2000 American Institute of Physics. [S0021-8979(00)09322-1]

I. INTRODUCTION

The modification of the elastic modulus of magnetic material by an applied dc magnetic field—the so called ΔE effect—has been known for a long time.¹ In the general case of bulk materials it is a rather complicated effect and there is little comprehensive description available in the literature. In this respect magnetic thin films or ribbons with an in-plane easy axis and first order uniaxial anisotropy constitute an interesting model system for a better understanding of the effect. Alternatively, the effect can be considered as a research or characterization tool for a better description of the film properties. It is well known that ferromagnetic amorphous materials exhibit, if any, only induced magnetic anisotropy. For instance, uniaxial anisotropy can be induced in thin films by heat treatment under an applied dc magnetic field or by being deposited under field. This has already been the subject of considerable fundamental work as well as the object of several practical applications.² The uniaxial anisotropy model of an amorphous film, with an easy axis in the film plane, is a well established one and is indeed a good predictive tool at least for a semiquantitative understanding of the magnetic behavior of a field annealed film or ribbon. In particular the model successfully predicts “first order” magnetic properties such as the static magnetization curves^{3,4} and the linear dynamical behavior.⁵ However, as the order of the property under consideration increases, the quality of the

predictions deteriorates in general. In this article we focus on the ΔE effect which is a rather high order property since it relates a variation of the elastic tensor to a field. A good deal of work has also been made on this effect mostly for amorphous ribbons.^{3,4,6-8} Comparatively little has been done, however, in thin films supported on substrates⁹ or similar structures.¹⁰ Here we report interesting experimental as well as theoretical results on the ΔE effect in thin films of the giant magnetostriction (GM) type with an induced in-plane easy axis.

Section II is devoted to the experimental aspects. Two types of films are studied, single layers of TbDyFeCo¹¹ and patented multilayer nanocomposite films formed from alternate high magnetization FeCo layers and high magnetostriction TbFeCo layers each being 6 nm thick.¹² The measurement method is described in some detail since, in contrast with previous studies, we measure the variations of the traction modulus and shear modulus. In addition, the moduli variations are measured for two orientations of the applied dc field, parallel and perpendicular to the easy axis.

Section III concerns the theoretical interpretation of the results. We show that the ideal uniaxial model gives at least a good semiquantitative understanding of the measured data. In particular the strong anomaly of the shear modulus in the hard axis bias configuration, best observed in nanocomposites, is linked to the divergence of the transverse magnetic susceptibility that is known to occur at a field equal to the anisotropy field. Deviations from the model are briefly discussed mainly in terms of misorientation and angular disper-

^{a)} Author to whom all correspondence should be addressed; electronic mail: sarkozi@phys.ubbcluj.ro

TABLE I. Basic properties of two typical samples.

Sample	Composition	Layers thickness (nm)	M_s (kA/m)	$\mu_0 H_c$ (mT)	$\mu_0 H_b$ (mT)	K_b (kJ/m ³)	b (MPa)	$b^2/2K_b$ (GPa)
Single layer	Tb _{0.36} Dy _{0.64}	1350	290	9.6	195	28.275	9.5	1.6
Multilayer	(Fe _{0.40} Co _{0.60}) _{1.27} Fe _{0.65} Co _{0.35} /Tb _{0.25} (Fe _{0.2} Co _{0.8}) _{0.75}	(6/6)×81	450	7.2	90	20.25	18	8

sion of the easy axis. Finally, an interesting and still not understood dissipation effect is observed.

II. EXPERIMENTS

Single layer and multilayer GM thin films were deposited by rf sputtering in an Ar atmosphere onto 100 or 150 μm thick (100) silicon substrates thereby forming a magnetoelastic bimorph. Single TbDyFeCo layers were deposited at a pressure of $2-5 \times 10^{-3}$ mbar and a rf power of 300 W using a composite target. Similar conditions were used for depositing the multilayered films but two targets were used and the substrate was moved sequentially from one to the other. Exact composition of the single layer and multilayer films are reported in Table I. The single layers thickness was typically 1300 nm whereas the multilayer films were formed by stacking alternatively 81 FeCo and TbFeCo layers, each typically 6 nm thick. The multilayer films were rendered magnetically anisotropic with a well defined in-plane easy axis by an annealing of the films (at 200 °C) under an external in-plane dc magnetic induction of 0.1 T. For the single layer films, the same result was obtained by applying an in-plane induction of 0.07 T during the deposition process itself. The films were then first characterized by tracing their in-plane static magnetization curves, using a vibrating sample magnetometer. From these plots, the spontaneous magnetization M_s , the coercive field H_c and the saturation field H_b were directly determined. A uniaxial anisotropy constant K_b was also determined—within the frame of the uniaxial first order anisotropy model—from the relation $K_b = \frac{1}{2}\mu_0 M_s H_b$. Here the index “b” stands for blocked, a reference to the fact that the film is actually clamped by its substrate.

For the magnetoelastic measurements, rectangular samples 2–5 mm wide and 10–15 mm long were then cut out of the bimorphs with the easy axis along the plate width. They were firmly glued at one end to a heavy base to form a simple cantilever structure. First the magnetoelastic coupling coefficient b was determined by a static method that has been widely reported elsewhere^{13–16,11} and which consists in measuring by an optical mean the cantilever curvature or torsion which is induced by a dc magnetic field. Table I summarizes the results of those static measurements obtained on two typical samples.

The dynamical measurements were then made on these same cantilever samples. The variations in the elastic moduli were deduced from analysis of the cantilever resonance frequencies. The mechanical resonances were excited electrostatically. A small brass electrode was placed off center behind the free end of the cantilever. Being off center, both

torsion and flexion resonance modes could be excited at the expense of efficiency in exciting the flexion mode. An ac voltage of 100 V root mean square was applied to the electrode at variable frequency. The electrostatic force generated was thus at twice this frequency. The deformations of the cantilever were measured optically as for the static b measurements. A two-dimensional position sensitive photodiode allowed both the flexion and torsion modes of resonance to be detected. The diode output was fed into a lock-in amplifier and the amplitude and phase of the resulting deformations were measured as a function of frequency. The phase variation $\Delta\phi$, in the vicinity of a resonance was measured and found to closely follow

$$\Delta\phi = \tan^{-1} \left[Q \left(\frac{f}{f_0} - \frac{f_0}{f} \right) \right],$$

as expected, where f_0 is the resonance frequency (assumed constant) and Q the quality factor. We observe typically $f_0 = 1-2$ kHz, $Q = 300-500$ for the flexural modes, and $f_0 = 6-12$ kHz and $Q = 1000-1500$ for the torsion modes. The use of phase measurements instead of amplitude measurements has the advantage of being insensitive to the excitation level. At a constant working frequency f , $\Delta\phi$ is also a function of f_0 . The phase variation for a given applied field H can thus be translated into a resonance frequency shift Δf_0 . From the relative frequency shift $\Delta f_0/f_0$ the relative variation of the effective elastic modulus of the film, ΔE_f was deduced using the relation

$$\Delta E_f = \frac{2}{3} \frac{h}{e} E_s \frac{\Delta f_0}{f_0},$$

where E_s is the substrate's relevant modulus, e the substrate thickness, and h the layer thickness. As will be explained below the effective modulus for the flexural mode is a planar traction modulus α (close to the Young's modulus) whereas for the torsion mode it is the planar shear modulus γ (which turns out to be equal to the bulk shear modulus usually noted as G). The results are presented on Figs. 1 and 2 together with theoretical fits that will be explained in the next section.

Figures 1(a) and 1(b) are deduced from the torsion resonance measurements on a single layer film and hence concern the shear modulus γ . They show $\Delta\gamma$ as a function of the dc field applied, respectively, along the easy axis (perpendicular to the cantilever length), and along the hard axis (parallel to the cantilever length). Note in particular the striking nonmonotonic character of the hard axis curve with its strong anomaly at $H = H_b$. Figure 1(c) is for the same sample but for the flexion mode and hence gives the variation $\Delta\alpha$ of the traction modulus α . Only the hard axis bias case needs to be

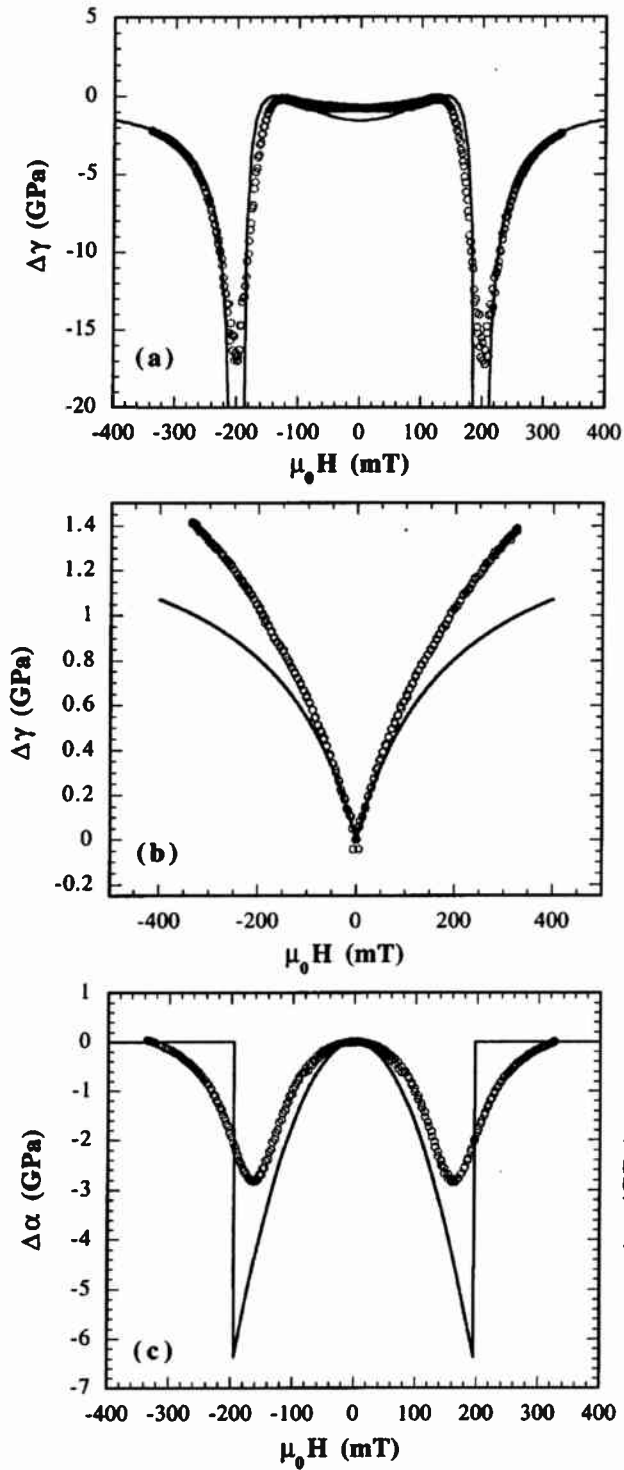


FIG. 1. Variation of elastic moduli for the single layer film: (a) shear modulus with field along hard axis; (b) shear modulus with field along easy axis; and (c) planar traction modulus with field along hard axis. In all cases the continuous line is the theoretical curve and the open circles are the experimental points.

illustrated here. Figures 2(a) and 2(b) again show the shear modulus for a film of FeCo/TbFeCo nanocomposite, and finally Fig. 2(c) gives the variation of traction modulus for the same sample and again, only for hard axis bias. Note the

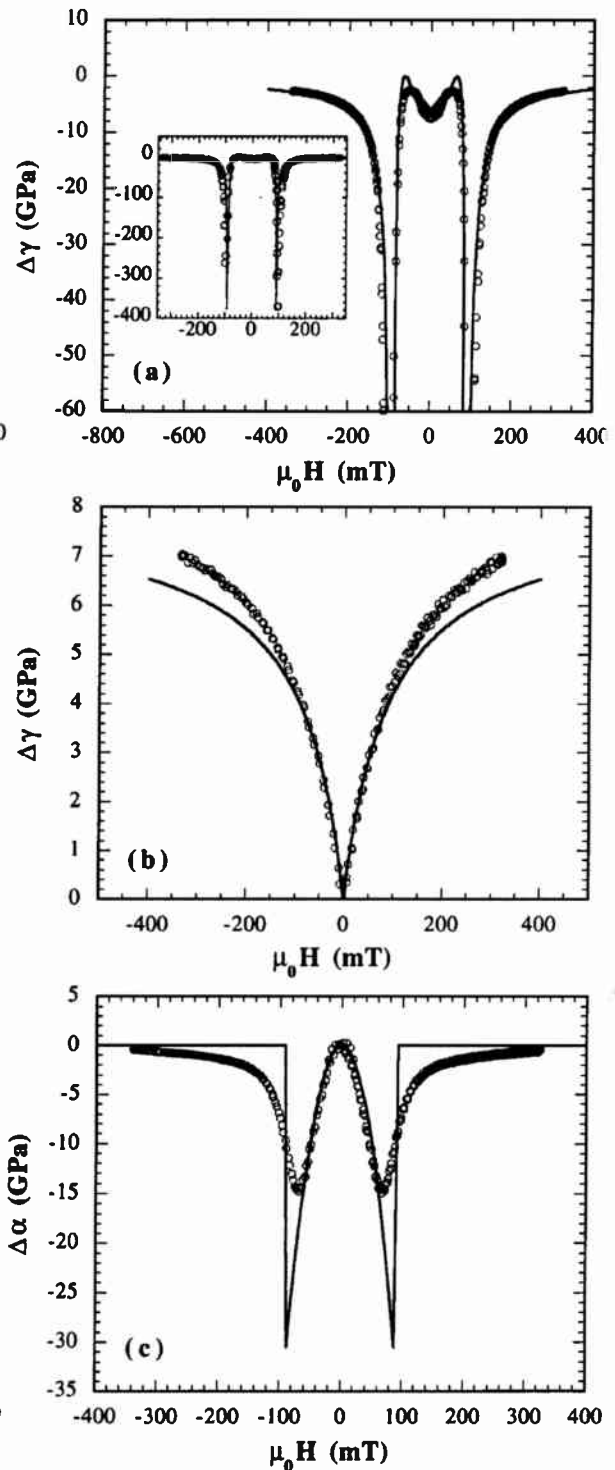


FIG. 2. Variation of elastic moduli for the multilayer film: (a) shear modulus with field along hard axis; (b) shear modulus with field along easy axis; and (c) planar traction modulus with field along hard axis. In all cases the continuous line is the theoretical curve and the open circles are the experimental points.

similarity with the corresponding curves of the single layer with however a much stronger anomaly in the vicinity of H_b .

Our measurement procedure of the resonance frequency

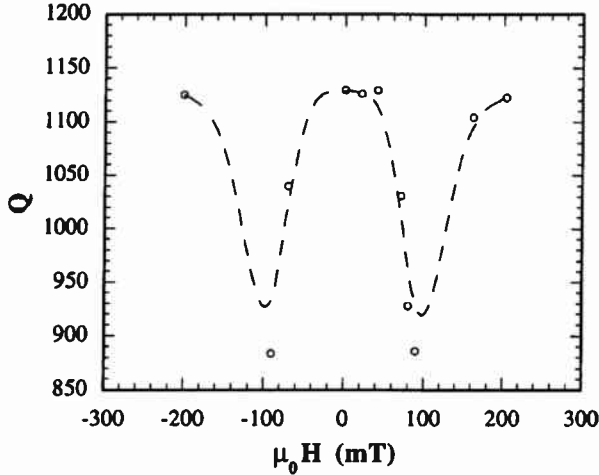


FIG. 3. Variation of the quality factor with field for the multilayer film. Open circles: experimental points. Broken line: guide for the eye.

shift relies on the assumption that the quality factor Q is independent of the applied bias. Although this is the expected behavior, we have checked this assumption by directly plotting the phase shift as a function of excitation frequency for each applied dc field. The results are illustrated by Fig. 3: it is seen that there is an anomaly in Q at $H = H_b$. The maximum variation observed amounts to 20% which is not sufficient to introduce serious errors in our results provided that the phase shifts remain small. Although this anomaly in Q is of minor importance for the ΔE measurements, it is very significant from the physical standpoint and this point will be discussed further below.

III. THEORETICAL CONSIDERATIONS AND DISCUSSION

We first define a rectangular axis system $Oxyz$ by taking Oz normal to the layer and Ox along the easy axis. The magnetic layer is assumed to be in a single domain state with the spontaneous magnetization \mathbf{M} along the easy axis Ox . This state is taken as the zero deformation and zero energy state. Other states are defined by θ , the angle between \mathbf{M} and Ox and the planar elastic deformations $S_1 = S_{xx}$, $S_2 = S_{yy}$ and $S_6 = S_{xy} = S_{yx}$. The free energy density function $F(\theta, S_1, S_2, S_6)$ can be quite straightforwardly written as

$$F = K_1 \sin^2 \theta - \mu_0 M_s (H_x \cos \theta + H_y \sin \theta) + \frac{1}{2} \alpha \{ [S_1 - S_1(\theta)]^2 + [S_2 - S_2(\theta)]^2 \} + \beta [S_1 - S_1(\theta)][S_2 - S_2(\theta)] + \frac{1}{2} \gamma [S_6 - S_6(\theta)]^2. \quad (1)$$

The first two terms represent the purely magnetic work that has to be supplied to the free (i.e., at zero stress) magnetic film to bring it from the state $\theta=0$ to state $\theta \neq 0$: K_1 is the uniaxial anisotropy constant of the free layer, H_x and H_y are the components of an applied dc field \mathbf{H} . During this process

the free magnetic layer suffers a spontaneous magnetostrictive strain having planar components $S_1(\theta)$, $S_2(\theta)$, $S_6(\theta)$. The following terms then express the mechanical work to be supplied to the material for changing from an intermediate state $(\theta, 0, 0)$ into a final state (θ, S_1, S_2, S_6) : α , β , and γ are the planar elastic moduli at constant magnetization (i.e., at constant θ). Assuming isotropic magnetostriction we can write the spontaneous magnetostrictive strains as

$$\begin{aligned} S_1(\theta) &= -S_0 \sin^2 \theta; \\ S_2(\theta) &= +S_0 \sin^2 \theta; \\ S_6(\theta) &= S_0 \sin 2\theta. \end{aligned} \quad (2)$$

Assuming further isotropic elastic behavior (at constant θ) it is easy to demonstrate the following relations:

$$\begin{aligned} \alpha &= \frac{E}{(1+\nu^2)}; \quad \beta = \frac{\nu E}{(1+\nu^2)}; \\ \gamma &= \frac{1}{2}(\alpha - \beta) = G; \quad G = \frac{E}{2(1+\nu)}, \end{aligned} \quad (3)$$

where E is the material's Young's modulus and G its shear modulus. Introducing the magnetoelastic coupling coefficient $b = (\alpha - \beta)S_0$, we finally get the following expression of the free energy density:

$$F = [K_1 + (\alpha - \beta)S_0^2] \sin^2 \theta + \mu_0 M_s (H_x \cos \theta + H_y \sin \theta) + \frac{1}{2} \alpha (S_1^2 + S_2^2) + \beta S_1 S_2 + \frac{1}{2} \gamma S_6^2 + b [(S_1 - S_2) \sin^2 \theta - \frac{1}{2} S_6 \sin 2\theta]. \quad (4)$$

Since our magnetic layers are very thin compared to their substrate, it can be assumed that they are not allowed to deform while reaching their new static equilibrium under applied dc field. Therefore, the equilibrium state satisfies the condition

$$S_1 = S_2 = S_6 = 0. \quad (5)$$

Let us now consider small variations $d\theta$, dS_1 , dS_2 , and dS_6 of the state variables around this new equilibrium state. Expanding the free energy (4) up to second order in $d\theta$, dS_1 , dS_2 and dS_6 , and taking into account equilibrium relations (5), we get

$$d^2 F = \frac{1}{2} \alpha (dS_1^2 + dS_2^2) + \frac{1}{2} \gamma dS_6^2 + \beta dS_1 dS_2 + b d\theta [(dS_2 - dS_1) \sin 2\theta - dS_6 \cos 2\theta] + [K_b \cos 2\theta + \frac{1}{2} \mu_0 M_s (H_y \sin \theta + H_x \cos \theta)] d\theta^2. \quad (6)$$

Here, we have introduced the anisotropy constant of the clamped film: $K_b = K_1 + (\alpha - \beta)S_0^2$. From Eq. (6), we get the following equations of state valid for small deviations from the equilibrium state:

$$\begin{aligned}
 dT_1 &= \alpha dS_1 + \beta dS_2 - \beta d\theta \sin 2\theta, \\
 dT_2 &= \beta dS_1 + \alpha dS_2 + \beta d\theta \sin 2\theta, \\
 dT_6 &= \gamma dS_6 - \beta d\theta \cos 2\theta, \\
 0 &= b[(dS_2 - dS_1) \sin 2\theta - dS_6 \cos 2\theta] \\
 &\quad + [2K_b \cos 2\theta + \mu_0 M_s (H_x \cos \theta + H_y \sin \theta)] d\theta,
 \end{aligned} \tag{7}$$

where dT_1 , dT_2 , and dT_6 are stress components. The last equation simply expresses that the sole field torque acting on magnetization is the static one due to H (no small signal field).

A. Field effect on shear modulus (torsion mode of the cantilever)

In the torsion measurement we can assume $dS_1 = dS_2 = 0$; this condition is actually imposed on the layer by its substrate. Therefore, we get

$$d\theta = \frac{b \cos 2\theta dS_6}{2K_b \cos 2\theta + \mu_0 M_s (H_x \cos \theta + H_y \sin \theta)}, \tag{8}$$

and the relevant shear modulus is

$$\begin{aligned}
 \frac{dT_6}{dS_6} &= \gamma - b \cos 2\theta \frac{d\theta}{dS_6} \\
 &= \gamma - \frac{b^2 \cos^2 2\theta}{2K_b \cos 2\theta + \mu_0 M_s (H_x \cos \theta + H_y \sin \theta)}.
 \end{aligned} \tag{9}$$

We first examine the case of the hard axis bias ($H_x = 0$; $H_y = H \neq 0$). In this case the equilibrium value of θ is known to be given by

$$\sin \theta = \frac{H}{H_b} = h, \tag{10}$$

where $h_b = 2K_b/M_s$ is the anisotropy field of the clamped layer, and h the reduced dc field. Equation (10) holds for $h < 1$. For $h > 1$, the solution is simply $\theta = \pi/2$. From Eqs. (9) and (10), we finally get, for $h < 1$,

$$\Delta\gamma = \frac{dT_6}{dS_6} - \gamma = -\frac{b^2}{2K_b} \frac{(1-2h^2)^2}{1-h^2}, \tag{11}$$

and for $h > 1$,

$$\Delta\gamma = -\frac{b^2}{2K_b} \frac{1}{h-1}. \tag{12}$$

The remarkable features of relations (11) and (12) are: (i) $\Delta\gamma$ is, as expected always negative, i.e., the free magnetization modulus is always smaller than the clamped magnetization modulus except when $\theta = 45^\circ$ and $h = 1/\sqrt{2}$, where $\Delta\gamma$ vanishes as the magnetization is not coupled to the torsion at this angle, (ii) a strong anomaly of $\Delta\gamma$ is predicted at $h = 1$. This will be further discussed below.

We now assume the bias field along the easy axis $H_y = 0$; $H_x = H$. Then, obviously $\theta = 0$ and we find after Eq. (9) that

$$\Delta\gamma = \frac{b^2}{2K_b} \frac{1}{h+1}. \tag{13}$$

B. Field effect on the transition modulus (flexural mode of the cantilever)

In the bending mode it can be assumed that $dS_6 = 0$ and $dS_2 = 0$. Although the first condition is always true for a cubic substrate, the second one follows from the particular orientation of the silicon cantilever axis (110) leading to a Poisson's ratio which is practically zero. Since it is obvious that there is no coupling between S_1 and a small rotation of magnetization in the case of easy axis bias, we treat only the case of hard axis bias. Following the same calculation procedure as above, we easily get the variation of the traction modulus $\Delta\alpha$:

$$\Delta\alpha = \frac{dT_1}{dS_1} - \alpha = -\frac{b^2}{2K_b} (4h^2). \tag{14}$$

Again this expression holds for $h < 1$. For $h > 1$, it is readily verified that

$$\Delta\alpha = 0. \tag{15}$$

Thus, $\Delta\alpha$ is discontinuous at $H = H_b$! Since the coupling between bending of the cantilever and layer magnetization rotation obviously vanishes when $H \geq H_b$, existence of a finite $\Delta\alpha$ just below H_b could seem a bit surprising. However this is due to the divergence of the transverse susceptibility when H approaches H_b . Just above H_b this susceptibility is finite but the coupling is strictly zero. This explains the discontinuity of $\Delta\alpha$.

C. Discussion

The theoretical relations (11)–(14), depend on three parameters, M_s , H_b , and b which are measured by static means (see Table I). These independently measured static parameters have been used to get the solid curves of Figs. 1 and 2. It is seen that there is an overall, at least semiquantitative agreement between theory and experiments. In particular the theoretical as well as experimental curves present notable features that deserve some comment.

The first remarkable feature regards the divergence of $\Delta\gamma$ that is predicted at $H = H_b$ in the hard axis bias configuration (G anomaly). This phenomenon shows up very clearly in the experiment on nanocomposite film even if $\Delta\gamma$ obviously remains finite. Although the exact absolute values of the shear modulus are not accurately known for our films (especially for our nanocomposite films) reasonable estimations can be made. For the nanocomposite we expect $\gamma = G \approx 20\text{--}50$ GPa whereas the experimental peak value of $\Delta\gamma$ approaches -400 GPa [see inset of Fig. 2(a)]. Therefore, there exists a small range of bias field centered at $H = H_b$ within which the G modulus is actually strongly negative! This range obviously corresponds to a region of elastic as well as magnetic bistability which should rather be studied by static experiments on free standing films or on cantilevers with a very thin substrate. The G anomaly is much weaker in the single layer film. There are at least two reasons for this. First, $b^2/2K_b$ is five times smaller than in the nanocomposite

(see Table I). Second, we have observed that the experiments in the hard axis bias configuration are rather sensitive to the orientation of the applied field with respect to the hard axis and even for the best alignment there remains the effect of a probable angular dispersion of the easy axis within the same sample. Therefore, the large magnitude of the measured G anomaly of the nanocomposite films suggests that the easy axis is extremely well defined in these films whereas the weaker G anomaly in the single layer film could result from some angular dispersion of the easy axis. A similar behavior has been observed for some time in the variation of the differential permeability as a function of a bias field¹⁷ (when plotting the easy axis permeability μ_{ea} against the bias field H applied along the hard axis), one should also observe a divergence at H_b after the ideal uniaxial anisotropy model. What is actually observed is rather a broad peak of μ_{ea} . Such rounding of the permeability divergence has been interpreted mainly in terms of spatial dispersion of the easy axis orientation.¹⁸ A second notable feature, at least in the theoretical curves, is the discontinuity of the planar traction modulus at $H=H_b$ again in the hard axis bias configuration. However, this predicted discontinuity is far from being observed in the experiments, this being true for both types of samples. Again we believe this to be the consequence of some angular dispersion of the easy axis or K_b values. Even at $h=1$, not all moments have $\theta=90^\circ$ and so a finite coupling still exists. Calculations by Squire^{6,7} show that only slight spatial dispersion of either the easy axis orientation or the anisotropy constant itself is actually sufficient to cause a pronounced rounding of the traction modulus discontinuity. Another experimental result that deserves comment is the anomaly of the Q factor that is observed at $H=H_b$ again in the hard axis bias configuration. Although it seems obvious that this anomaly must be related to the magnetic dissipation in the alloy film, we have, at present, no satisfactory explanation for this effect. The effect of a static field on the mechanical damping of bulk materials has been already reported by several workers^{19–21} and is known as the magnetomechanical damping effect. In particular the behavior of amorphous wires reported by Squire *et al.*²⁰ closely resembles our observations (see Fig. 17 of Ref. 20). Although two main theoretical models have already been derived,^{22,23} further work is needed to see whether these models also apply to thin film materials. Finally, it is worth commenting on the pole effect:¹⁵ it is due to the magnetostatic restoring force on the cantilever that arises when the field is along the cantilever axis. The pole effect has sometimes been mistaken with the ΔE effect. In our studies the pole effect is around 100 times smaller than the variations shown here.

IV. CONCLUSION

The ΔE effect has been measured in substrate supported thin films of giant magnetostrictive material by means of a resonance method. Both torsion and bending modes of a test cantilever were used to plot the variations of shear modulus as well as traction modulus of the films, against dc field applied in the film plane. The dc field was either parallel or perpendicular to the magnetic easy axis of the layers. Two kinds of magnetostrictive material were studied, a single layer of composition TdDyFeCo and a nanocomposite multilayer of FeCo and TbFeCo layers, each typically 6 nm thick. Our study demonstrates a good semiquantitative agreement between experiments and the simple model of uniaxial first order anisotropy. In particular the strong G anomaly predicted by the model for the hard axis bias configuration shows up very nicely in the nanocomposite films. Finally, an interesting and still not understood mechanical dissipation anomaly has been observed in the torsional resonance of our magnetostrictive bimorphs. In our opinion these experiments also open up very interesting possibilities in sensor applications.

¹E. du Trémolet de Lacheisserie, *Magnetostriction* (CRC, Cleveland, OH, 1993).

²D. A. Thompson, L. T. Romankiw, and A. F. Madayas, *IEEE Trans. Magn.* **11**, 1039 (1975).

³M. L. Spano, K. B. Hathaway, and H. T. Savage, *J. Appl. Phys.* **53**, 2667 (1982).

⁴J. D. Livingston, *Phys. Status Solidi A* **70**, 591 (1982).

⁵G. Perrin, O. Acher, J. C. Peuzin, and N. Vukadinovic, *J. Magn. Magn. Mater.* **157–158**, 289 (1996).

⁶P. T. Squire, *J. Magn. Magn. Mater.* **87**, 299 (1990).

⁷P. T. Squire, *J. Magn. Magn. Mater.* **140–144**, 1829 (1995).

⁸J. Gutiérrez, A. Garcia-Arribas, J. S. Garitaonandia, and J. M. Barandiaran, *J. Magn. Magn. Mater.* **157–158**, 543 (1996).

⁹Q. Su, J. Morillo, Y. Wen, and M. Wuttig, *J. Appl. Phys.* **80**, 3604 (1996).

¹⁰D. Atkinson and P. Duhaj, *J. Magn. Magn. Mater.* **157–158**, 156 (1996).

¹¹D. Givord, J. Betz, N. H. Duc, K. Mackay, and E. du Trémolet de Lacheisserie, *Proceedings of the Second International Workshop of Materials Science, Hanoi, Vietnam, 1996*, p. 287.

¹²E. Quandt, A. Ludwig, D. Givord, K. Mackay, and J. Betz, German patent, Deutsches Patentamt, München No. 196 21 166.2 (1996).

¹³A. C. Tam and H. Schröder, *IEEE Trans. Magn.* **25**, 2629 (1989).

¹⁴E. Kloholm, *IEEE Trans. Magn.* **12**, 819 (1976).

¹⁵E. du Trémolet de Lacheisserie and J. C. Peuzin, *J. Magn. Magn. Mater.* **136**, 189 (1994).

¹⁶R. Watts, M. R. J. Gibbs, W. J. Karl, and H. Szymczak, *Appl. Phys. Lett.* **70**, 2607 (1997).

¹⁷E. Feldtkeller, *Z. Phys.* **176**, 510 (1963).

¹⁸H. Hoffmann, *Status Solidi* **33**, 175 (1969).

¹⁹R. Becker and M. Kornetzki, *Z. Phys.* **88**, 634 (1934).

²⁰P. T. Squire, D. Atkinson, and S. Atalay, *IEEE Trans. Magn.* **31**, 1239 (1995).

²¹S. Atalay and P. T. Squire, *J. Appl. Phys.* **73**, 871 (1993).

²²G. W. Smith and J. R. Birchak, *J. Appl. Phys.* **40**, 5174 (1969).

²³J. Degauque and B. Astie, *Phys. Status Solidi A* **59**, 805 (1980).